Macromolecules

Note

pubs.acs.org/Macromolecules

Polystyrene-*block*-poly(ethylene oxide) Reverse Micelles and Their Temperature-Driven Morphological Transitions in Organic Solvents

Lian Wang,[†,‡] Xinfei Yu,[†,*] Shuguang Yang,[†] Joseph X. Zheng,[†] Ryan M. Van Horn,[†] Wen-Bin Zhang,[†] Junting Xu,[‡,*] and Stephen Z. D. Cheng[†,*]

[†]Department of Polymer Science, College of Polymer Science and Polymer Engineering, The University of Akron, Akron, Ohio 44325-3909, United States

[‡]MOE Key Laboratory of Macromolecular Synthesis and Functionalization, Department of Polymer Science and Engineering, Zhejiang University, Hangzhou 310027, China

Supporting Information

INTRODUCTION

It has been widely reported that amphiphilic diblock copolymers can self-assemble into micelles when selective solvent is added into copolymer solution with its common solvent above the critical micelle concentration (CMC) of the copolymer.[1−12] For amphiphilic diblock copolymers containing water-soluble blocks, various nanoscale morphologies in aqueous solution such as sphere, cylinder, and vesicle and their transformations have been extensively investigated due to their potential biomedical applications.[13−15] Generally speaking, formation of micelles of block copolymers in solution could be controlled by the molecular architecture, the size of each block, polymer concentration, etc.[16,17] Micellar morphologies of block copolymers could be affected by the solvent quality, the solvent/nonsolvent ratio, the polymer concentration, the pH value, additives such as salts, ions, and homopolymer, and/or the temperature.[18−22] Theoretical calculations of micelle free energies were conducted to predict and explain those morphological formations based on mean-field theory in thermodynamic equilibrium. A micelle's free energy is commonly attributed to the free energy of the core, F_{core}, the free energy of the interface, $F_{interface}$, and the free energy of the corona, F_{corona}. Micelle morphology with a lower overall free energy would be more stable under one set of specific experimental conditions.[23,24] On the other hand, the formation of diblock copolymer micelles containing water-soluble blocks in organic solvent (reverse micelles) has also received a variety of attention due to their applications in encapsulation and as nanoreactors.[25−27] The transformation of reverse micelles so far, however, has been rare due to the difficulties of tuning the solvent properties.

Micellization of polystyrene-*block*-poly(ethylene oxide) (PS-*b*-PEO) in a selective solvent was first observed several decades ago.[3] Recently, micellization and morphological transitions of an asymmetric PS-*b*-PEO block copolymer in *N*,*N*-dimethylformamide (DMF)/water and DMF/acetonitrile was systematically studied in our previous work.[21,28,29] Micellar morphologies were found to be dependent on the water content and polymer concentrations. Furthermore, temperature was found to drive the micellar morphologies in DMF/water mixtures. With an increase in temperature, morphological changes were observed from vesicles to worm-like cylinders and then to spheres. In this letter, reverse micelles of PS-*b*-PEO were investigated in mixed organic solvents, in which 1,4-dioxane was utilized as the common solvent and cyclohexane was the selective solvent. The reverse micelles contain PEO blocks as the micellar core and PS blocks as the corona. The effect of temperature on the micellar morphological changes was further investigated. Transmission electron microscopy (TEM) and light scattering (LS) experiments were conducted to study the micellar morphologies and their transformation process. Finally, the origin of morphological changes with temperature was illustrated by the free energy calculation of micelles as a first approximation.

EXPERIMENTAL SECTION

Materials and Preparation of Micelle Solutions. A diblock copolymer PS_{164}-*b*-PEO_{827} was purchased from Polymer Source Inc. The degrees of polymerization for the PS and PEO blocks are 164 and 827, respectively. The M_n, M_w, and polydispersity of this diblock copolymer, characterized by size exclusion chromatography, were 52.8 kg/mol, 56.0 kg/mol, and 1.06, respectively. The M_ns of the PS and PEO blocks were calculated utilizing nuclear magnetic resonance experiments to be 16.4 kg/mol and 36.4 kg/mol, respectively. The volume fraction of the PEO blocks was 0.76.

This PS_{164}-*b*-PEO_{827} was first dissolved in 1,4-dioxane with stirring at room temperature for one day and filtered through a 0.2 μm filter before using. Cyclohexane was filtered through a 0.2 μm filter and then slowly added into the polymer solution (with a rate of 0.01 mL/min) with vigorous stirring. After reaching the preset 1,4-dioxane/cyclohexane ratio, solutions were held with mild stirring at room temperature for 3 days until equilibrium was reached. Equilibrated micellar solutions were kept standing without stirring for 1 day before morphological observations by TEM. For studying the temperature effect on the morphological transitions, the micellar solutions in vials were kept at the desired temperature in a temperature-controlled oil bath equipped with a digital temperature controller having an accuracy of ±0.1 °C. During cooling, the micellar solutions were equilibrated at the preset temperature for at least 12 h before morphological observations.

Instruments and Characterizations. Observations of micelle morphology were conducted on a Philips TECNAI TEM with an accelerating voltage of 120 kV. The micelle solution was quenched into excess cyclohexane to fix the micellar morphologies. A drop of quenched micellar solution was placed on the carbon-coated grid.

Received: February 10, 2012
Revised: April 1, 2012
Published: April 9, 2012

dx.doi.org/10.1021/ma3002752 | *Macromolecules* 2012, 45, 3634−3638

Excess solution was removed with filter paper after a few minutes. The grids were then dried at room temperature and atmospheric pressure for at least one day before TEM observation. Owing to the high glass transition temperature of the PS blocks after the solvent drying and severe restriction of PEO block mobility in selective solvent, the micellar morphology could be fixed on the grids during solvent evaporation.

Dynamic and static light scattering (DLS and SLS) experiments were carried on a Brookhaven Instrument coupled with a BI-200SM goniometer and BI-9000AT correlator. An EMI-9863 photo multiplier tube is used for photon counting. A Meller Griot 35 mW He−Ne laser was utilized as the light source with wavelength 632.8 nm. A cylindrical glass scattering cell (with a diameter of 12 mm) was positioned at the center of a thermostated bath (with an accuracy of the temperature control at ±0.01 °C) using decahydronaphthalene for refractive index matching. The measurements were carried out at a 90° scattering angle. The glass scattering cells were thoroughly cleaned by ultrasonication in THF and acetone to eliminate any dust and impurity.

RESULTS AND DISCUSSION

Reverse Micelles of PS_{164}-*b*-PEO_{827} Block Copolymers. In this study, 1,4-dioxane was chosen as the common solvent, and cyclohexane was selected as the selective solvent. PS_{164}-*b*-PEO_{827} was first dissolved in 1,4-dioxane with an initial polymer concentration of 0.5 (wt) %. Cyclohexane was added very slowly until the final cyclohexane concentration reached 80 (wt) %, and the final concentration of PS_{164}-*b*-PEO_{827} was 0.1 (wt) %. Figure 1a shows a TEM bright field (BF) image of spherical micelles of PS_{164}-*b*-PEO_{827}. Figure 1b shows dynamic light scattering results of the spherical micelles. The DLS results indicate that the apparent hydrodynamic diameter of the spherical micelles ($D_{h,app}$) is centered at 49 nm, which is larger than the size observed by TEM (28.4 nm, Figure 1a). This is probably due to the collapse of the micelles (especially the coronas) caused by solvent evaporation during TEM sample preparation. By combining DLS and TEM results, the spherical morphology were confirmed to be the authentic aggregation form in the micelle solution.

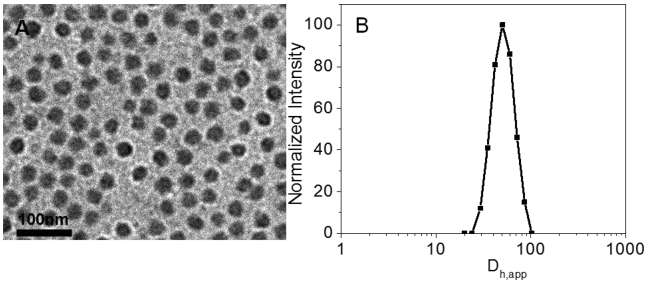

Figure 1. (a) TEM BF image of spherical micelles of PS_{164}-*b*-PEO_{827}. (b) Size distribution of spherical micelles after CONTIN analysis of the DLS results.

Temperature-Induced Morphological Transition of Micelles. Temperature dependent experiments were conducted in a thermal bath with a precision of ±0.1 °C. The micelle solutions were kept at the preset temperatures for more than 3 h and monitored by DLS experiments. When the light scattering intensities reached a constant, the micelle solutions were then used for TEM sample preparation (assuming that the morphological change is completed and that the solution is now under thermodynamic equilibrium). Figure 2 illustrates the dependence of light scattering intensity with temperature during cooling for the micelle solution with 80 (wt) % cyclohexane at 0.1 (wt) % PS_{164}-*b*-PEO_{827}. A sharp change in the scattering intensity has been observed within a temperature range of 0 °C < T < 10 °C. This sharp increase in scattering intensity reflects the existence of a micellar morphological transformation. The variation of apparent hydrodynamic diameter ($D_{h,app}$) has also been included in Figure 2. The value of $D_{h,app}$ increases from 50 to 168 nm when the temperature decreases from +25 to −10 °C, which corresponds to the scattering intensity change. Below −10 °C, the intensity does not substantially change until the lowest temperature available for experiments, −25 °C, is reached. At such a low temperature, it is expected that the diblock copolymer may possess little mobility. The larger value of $D_{h,app}$ suggests that a new association with a larger size may be constructed when decreasing the temperature.

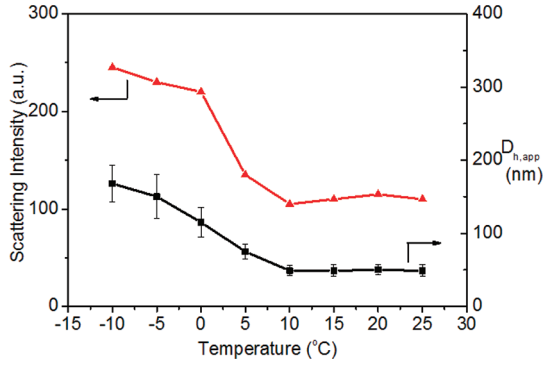

Figure 2. Light scattering intensity (red) and apparent hydrodynamic diameter (black) of PS_{164}-*b*-PEO_{827} as a function of temperature.

Figure 3 shows a set of TEM BF images of the micellar morphologies during the cooling process. At room temperature (25 °C), spherical micelles are formed as shown in Figure 1a. A mixture of spherical micelles and cylindrical micelles are observed in Figure 3a when the temperature decreased to 5 °C; however, spherical micelles remain the majority. Further decreasing the temperature to 0 °C, the micellar morphology changed into pure cylinders (Figure 3b). The micelle morphology further evolved into a mixture of vesicles and cylinders at −5 °C (Figure 3c).

Micelle Free Energy Calculations. The driving force for micelle formation and morphological transformations is the tendency to minimize the overall micelle free energy under a specific set of experimental conditions. The overall micelle free energy can be expressed as[23]

$$F = F_{core} + F_{interface} + F_{corona} \quad (1)$$

where the term F_{core} is the free energy of the core that involves deformation of the core block conformations such as stretching or compressing, leading to deviation from its random coil conformation. In this case, this corresponds to the PEO block. The term $F_{interface}$ is determined by the surface tension between the core and solvent at the interface. The term F_{corona} relates to the steric and electrostatic (if ionic block exists, however that is not the case here) interactions between corona blocks and solvent. Here, it is the PS block.

F_{core} can be correlated to the degree of stretching or compression (S_c) of the PS blocks in the core and calculated as[18]

$$S_c = R_{core}/R_0 \quad (2)$$

dx.doi.org/10.1021/ma3002752 | Macromolecules 2012, 45, 3634−3638

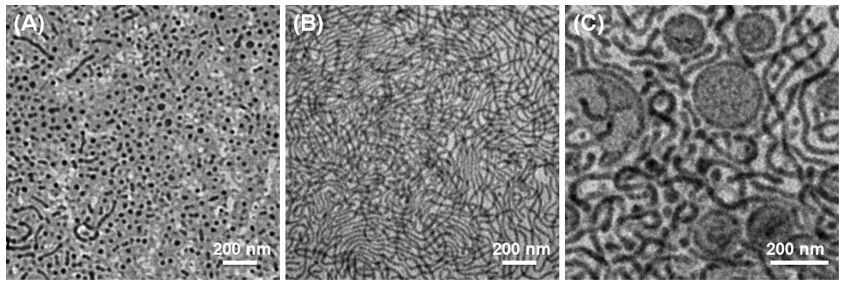

Figure 3. Morphology transition of PS_{164}-*b*-PEO_{827} on cooling for a micelle solution with 0.1 (wt) % polymer concentration at 80 (wt) % cyclohexane content in dioxane/cyclohexane system: (a) mixture of spheres and cylinders at 5 °C; (b) pure cylinders at 0 °C; (c) mixture of vesicles and cylinders at −5 °C.

Table 1. Physical Parameters and Free Energy Calculations of Reverse Micelles at Three Different Temperatures

temp (°C)	morph.	$R_{core}(nm)^a$	$S_c{}^b$	$s(nm^2)^c$	F_{core}/kT	$F_{interface}/kT$	F_{corona}/kT	$F_{overall}/kT$
25	sphere	14.2 ± 1.0	0.79 ± 0.06	12.0 ± 0.8	0.6 ± 0.1	30.3 ± 2.0	2.2 ± 0.1	33.1 ± 2.2
0	cylinder	12.0 ± 0.6	0.67 ± 0.03	9.5 ± 0.5	1.4 ± 0.1	25.6 ± 1.3	2.8 ± 0.3	29.8 ± 1.7
−5	vesicle	8.4 ± 0.4	0.47 ± 0.02	6.8 ± 0.4	5.6 ± 0.5	18.6 ± 1.1	4.0 ± 0.5	28.2 ± 2.1

[a] R_{core} is the diameter of spherical and cylindrical micelles and half of wall thickness for vesicles. [b] S_c is the degree of stretching of PEO blocks in the micellar core. [c] *s* is the interfacial area per chain.

where R_{core} is the radius of the PEO core in the spherical and cylindrical micelles. In the case of vesicles, half of the wall thickness was utilized as R_{core}. The quantity R_0 is the unperturbed end-to-end distance of the PEO chain which can be calculated from the equation[30]

$$R_0 = 0.094(M)^{0.5} \tag{3}$$

where M is the number-average molecular weight of the PEO blocks. The value of R_0 is calculated to be 17.9 nm when the PEO block's molecular weight is 36.4 kg/mol.

As a result, the PEO blocks are slightly compressed in the core of the spherical micelle with an average R_{core} of 14.2 nm. The average R_{core} of the cylindrical micelles is found to be 12.0 nm, reflecting a higher degree of compression of the PEO blocks. The PEO block has the highest degree of compression in the vesicles with an average R_{core} of 8.4 nm. The calculated values of S_cs are listed in Table 1, which decreases from 0.79 for spheres to 0.47 for vesicles. Therefore, the free energy of compressed PEO blocks in the micellar core can be calculated based on the following equation:[28]

$$F_{core}/(kT) = k_j(1/S_c)^2 \quad (S_c < 1) \tag{4}$$

Here, k_j is the numerical coefficients of a dense PEO core: $j = 1$ for lamella, $k_1 = \pi^2/8$; $j = 2$ for cylinder, $k_2 = \pi^2/16$; and $j = 3$ for sphere, $k_3 = 3\pi^2/80$. The calculated free energy of the micellar core increases from 0.6 kT for spheres to 5.6kT for the vesicles with highest compressibility.

The second term, $F_{interface}$, relates to the interfacial free energy between the core (PEO) blocks at the interface and the solvents. Therefore

$$F_{interface} = \gamma s \tag{5}$$

where s is the interfacial area per chain, and γ is surface tension, which is related to $\chi_{PEO-solvent}$ described by the following equation:

$$\gamma = (kT/a_{PEO}{}^2)(\chi_{PEO-solvent}/6)^{0.5} \tag{6}$$

where a_{PEO} is the length of a PEO monomer. The term $\chi_{PEO-solvent}$ is dependent on temperature as follows:[31]

$$\chi_{PEO-solvent} = \alpha + \frac{\beta}{T} \tag{7}$$

where α and β are constants depending on the solvent properties. It was deduced from experimental data that $\alpha = -0.84$ and $\beta = 565$ (see Supporting Information).[32,33] The value of $\chi_{PEO-solvent}$ is thus highly temperature dependent, and it changes from 1.06 at 25 °C to 1.27 at −5 °C.

The interfacial area per chain (s_j) can be calculated based on the following equation:

$$s_j = jV_{PEO}N_{PEO}/(fR_{core}) \tag{8}$$

where $j = 1$ for lamella, $j = 2$ for cylinder, and $j = 3$ for sphere; V_{PEO} is the volume of the PEO monomer, N_{PEO} is the degree of polymerization of the PEO blocks, and f is the volume fraction of the PEO blocks in the core which may be treated as unity due to the high content of selective solvent, driving the PEO chains to pack densely to avoid interaction with selective solvent. The calculated values of $F_{interface}$ are listed in Table 1 and decrease from 30.3 kT for spheres to 18.6 kT for vesicles.

The third term, F_{corona}, is based on the expression proposed by Zhulina et al. in their theory of diblock copolymer micelles.[24] The corona could be treated as chains tethered on a planar substrate when the corona is much shorter than the core block. This free energy is expressed by:

$$F_{corona}/(kT) = \hat{C}_H\hat{C}_F N_{PS}(sa_{PS}{}^{-2})^{-1/2\nu} \tag{9a}$$

where N_{PS} is the degree of polymerization of PS block and a_{PS} is the PS monomer length. Cyclohexane is a θ-solvent for the PS blocks at a critical temperature of 34.5 °C. The mixed solvent may be recognized as an approximate θ-solvent when the content of cyclohexane reaches 80%. Therefore, ν, the scaling exponent, is equal to 0.5. The $\hat{C}_H$ and $\hat{C}_F$ values are numerical prefactors, and in the case of Θ-solvent, they are

$$\hat{C}_H = 0.68(l/a_{PS})^{1/4} \tag{9b}$$

$$\hat{C}_F = 1.38(l/a_{PS})^{-3/4} \tag{9c}$$

dx.doi.org/10.1021/ma3002752 | *Macromolecules* 2012, 45, 3634−3638

where l is the Kuhn length of PS. The calculated values of F_{corona} increases from 2.2 kT for spheres to 4.0 kT for vesicles as shown in Table 1.

The change of free energy for different micellar morphologies can be estimated based on calculations above. During the cooling process, $\chi_{PEO-solvent}$ increases up to 20% and leads to an increase of the surface tension between the PEO core bock and solvents. Spherical morphologies with the highest surface area become unfavorable and transfer to cylinders and finally to vesicles. F_{core}/kT and F_{corona}/kT increase due to the increased compressibility and crowding for the micellar PEO core blocks and PS corona blocks, respectively. These two free energy terms, however, are balanced by the reduction of $F_{interface}/kT$, which is dominant. Therefore, the overall free energy of the micelles decreases from spheres to cylinders and to vesicles with a reduction in temperature as shown in Table 1.

Although the interfacial free energy is demonstrated to be the main driving force for the morphology transitions induced by decreasing temperature in this system, it is surprising that the reversible transformations when increasing to room temperature is not able to be observed in our experimental time range (24 h). This may be due to the transition kinetics possessing a large hysteresis. It is thus speculated that both blocks are so restricted under these solvent and temperature conditions that the morphological transformations may take a much longer time to occur during heating to room temperature. As such, the recovery of those micellar morphologies after the transformations require a substantially longer period of time compared with our current experimental conditions. This surprising observation and a three-dimensional morphological phase diagram combining the polymer concentration, solvent composition and temperature are still under investigations to understand the morphological transformation mechanism for these reverse micelles.

CONCLUSION

In summary, reverse micelles with PEO blocks as the micelle cores and PS blocks as the micelle corona have been obtained by dissolving PS_{164}-b-PEO_{827} in 1,4-dioxane and slowly adding selective solvent (cyclohexane). Reverse spherical micelles formed at a cyclohexane content of 80 (wt) % at room temperature. The effects of temperature on the micellar morphologies have been investigated. TEM and DLS experimental observations have shown that pure spherical micelles transformed into a mixture of spheres and cylinders at 5 °C. Uniform cylindrical micelles formed at 0 °C. A mixture of cylinders and vesicles appeared as temperature decreased to −5 °C. As a first approximation, the free energies of micelles with various morphologies were calculated to understand the thermodynamic reasons for the morphological transformations. The results revealed that the $F_{interface}$ term dominates the morphology transformations due to the specific fact that $\chi_{PEO-solvent}$ is highly temperature dependent.

ASSOCIATED CONTENT

Supporting Information

Calculations of $\chi_{PEO-solvent}$, a table of solubility parameters and calculated $\chi_{PEO-solvent}$, and a figure showing the dependence of $\chi_{PEO-solvent}$ on temperature. This material is available free of charge via the Internet at http://pubs.acs.org.

AUTHOR INFORMATION

Corresponding Author

*E-mail: (S.Z.D.C.) scheng@uakron.edu. Telephone: +1-330-972-6931. (X.Y.) E-mail: xy5@uakron.edu. Telephone: +1-330-972-8281. (J.X.) E-mail: xujt@zju.edu.cn. Telephone: +86-571-87953164.

Notes

The authors declare no competing financial interest.

ACKNOWLEDGMENTS

This work was supported by the Division of Materials Research at the National Science Foundation (DMR-0906898). Dr. Xu would like to thank the financial support from the National Foundation of China (20974099) and State Key Laboratory of Chemical Engineering. Lian Wang acknowledges her support from the Chinese Scholarship Council.

REFERENCES

(1) Evans, F.; Wennerstrom, H. *The colloidal domain: where physics, chemistry, biology, and technology meet*, 2nd ed.; Wiley-VCH: New York, 1999.
(2) de Gennes, P. G. *Macromolecules* **1980**, *13*, 1069−1075.
(3) Wilhelm, M.; Zhao, C. L.; Wang, Y.; Xu, R.; Winnik, M. A.; Mura, J. L.; Riess, G.; Croucher, M. D. *Macromolecules* **1991**, *24*, 1033−1040.
(4) Prochazka, K.; Kiserow, D.; Ramireddy, C.; Tuzar, Z.; Munk, P.; Webber, S. E. *Macromolecules* **1992**, *25*, 454−460.
(5) Wu, G.; Chu, B. *Macromolecules* **1994**, *27*, 1766−1773.
(6) Zhang, L.; Eisenberg, A. *Science* **1995**, *268*, 1728−1731.
(7) Chen, E.-Q.; Xia, Y.; Graham, M. J.; Foster, M. D.; Mi, Y.; Wu, W.-L.; Cheng, S. Z. D. *Chem. Mater.* **2003**, *15*, 2129−2135.
(8) Liu, X.; Kim, J.-S.; Wu, J.; Eisenberg, A. *Macromolecules* **2005**, *38*, 6749−6751.
(9) Duxin, N.; Liu, F.; Vali, H.; Eisenberg, A. *J. Am. Chem. Soc.* **2005**, *127*, 10063−10069.
(10) Bang, J.; Jain, S.; Li, Z.; Lodge, T. P.; Pedersen, J. S.; Kesselman, E.; Talmon, Y. *Macromolecules* **2006**, *39*, 1199−1208.
(11) Du, B.; Mei, A.; Yin, K.; Zhang, Q.; Xu, J.; Fan, Z. *Macromolecules* **2009**, *42*, 8477−8484.
(12) Jain, S.; Bates, F. S. *Science* **2003**, *300*, 460−464.
(13) Rösler, A.; Vandermeulen, G. W. M.; Klok, H.-A. *Adv. Drug. Deliver, Rev.* **2001**, *53*, 95−108.
(14) Kataoka, K.; Harada, A.; Nagasaki, Y. *Adv. Drug. Deliver, Rev.* **2001**, *47*, 113−131.
(15) Fuks, G.; Mayap Talom, R.; Gauffre, F. *Chem. Soc. Rev.* **2011**, *40*, 2475−2493.
(16) Zhou, Z.; Li, Z.; Ren, Y.; Hillmyer, M. A.; Lodge, T. P. *J. Am. Chem. Soc.* **2003**, *125*, 10182−10183.
(17) Förster, S.; Antonietti, M. *Adv. Mater.* **1998**, *10*, 195−217.
(18) Zhang, L.; Eisenberg, A. *J. Am. Chem. Soc.* **1996**, *118*, 3168−3181.
(19) Shen, H.; Eisenberg, A. *J. Phys. Chem. B* **1999**, *103*, 9473−9487.
(20) Liu, F.; Eisenberg, A. *J. Am. Chem. Soc.* **2003**, *125*, 15059−15064.
(21) Yang, S.; Yu, X.; Wang, L.; Tu, Y.; Zheng, J. X.; Xu, J.; Van Horn, R. M.; Cheng, S. Z. D. *Macromolecules* **2010**, *43*, 3018−3026.
(22) Yu, X.; Zhong, S.; Li, X.; Tu, Y.; Yang, S.; Van Horn, R. M.; Ni, C.; Pochan, D. J.; Quirk, R. P.; Wesdemiotis, C.; Zhang, W.-B.; Cheng, S. Z. D. *J. Am. Chem. Soc.* **2010**, *132*, 16741−16744.
(23) Zhang, L.; Eisenberg, A. *Polym. Adv. Technol.* **1998**, *9*, 677−699.
(24) Zhulina, E. B.; Adam, M.; LaRue, I.; Sheiko, S. S.; Rubinstein, M. *Macromolecules* **2005**, *38*, 5330−5351.
(25) Alexandridis, P.; Andersson, K. *J. Phys. Chem. B* **1997**, *101*, 8103−8111.
(26) Eastoe, J.; Hollamby, M. J.; Hudson, L. *Adv. Colloid Interface Sci.* **2006**, *128−130*, 5−15.

(27) Van Horn, W. D.; Ogilvie, M. E.; Flynn, P. F. *J. Am. Chem. Soc.* **2009**, *131*, 8030−8039.
(28) Bhargava, P.; Zheng, J. X.; Li, P.; Quirk, R. P.; Harris, F. W.; Cheng, S. Z. D. *Macromolecules* **2006**, *39*, 4880−4888.
(29) Bhargava, P.; Tu, Y.; Zheng, J. X.; Xiong, H.; Quirk, R. P.; Cheng, S. Z. D. *J. Am. Chem. Soc.* **2007**, *129*, 1113−1121.
(30) Rubinstein, M.; Colby, R. H. *Polymer Physics*, 1st ed.; Oxford University Press: London, 2003.
(31) Barton, A. F. M., *Handbook of Polymer-Liquid Interaction Parameters and Solubility Parameters*. CRC Press: Boston, MA, 1990.
(32) Monique, G. *Polymer* **1983**, *24*, 865−870.
(33) Fernández-Berridi, M. J.; Martin; Guzmán, G.; Iruin, J. J.; Elorza, J. M. *Polymer* **1983**, *24*, 417−422.